

# Temperature dependent vibrational lifetimes in supercritical fluids near the critical point

D. J. Myers, Shirley Chen, Motoyuki Shigeiwa, Binny J. Cherayil,<sup>a)</sup> and M. D. Fayer<sup>b)</sup>  
*Department of Chemistry, Stanford University, Stanford, California 94305*

(Received 8 May 1998; accepted 10 July 1998)

Vibrational relaxation measurements on the CO asymmetric stretching mode ( $\sim 1980\text{ cm}^{-1}$ ) of tungsten hexacarbonyl ( $\text{W}(\text{CO})_6$ ) as a function of temperature at constant density in several supercritical solvents in the vicinity of the critical point are presented. In supercritical ethane, at the critical density, there is a region above the critical temperature ( $T_c$ ) in which the lifetime increases with increasing temperature. When the temperature is raised sufficiently ( $\sim T_c + 70\text{ }^\circ\text{C}$ ), the lifetime decreases with further increase in temperature. A recent hydrodynamic/thermodynamic theory of vibrational relaxation in supercritical fluids reproduces this behavior semiquantitatively. The temperature dependent data for fixed densities somewhat above and below the critical density is in better agreement with the theory. In fluoroform solvent at the critical density, the vibrational lifetime also initially increases with increasing temperature. However, in supercritical  $\text{CO}_2$  at the critical density, the temperature dependent vibrational lifetime decreases approximately linearly with temperature beginning almost immediately above  $T_c$ . The theory does not reproduce this behavior. A comparison between the absolute lifetimes in the three solvents and the temperature trends is made. © 1998 American Institute of Physics. [S0021-9606(98)51938-1]

## I. INTRODUCTION

In this paper vibrational lifetime measurements on the asymmetric CO stretching mode ( $T_{1u}$ ;  $\sim 1980\text{ cm}^{-1}$ ) of tungsten hexacarbonyl ( $\text{W}(\text{CO})_6$ ) in supercritical ethane, fluoroform, and  $\text{CO}_2$  solvents are presented and analyzed. The measurements are made at constant density as a function of temperature for several densities at and near the critical density. The qualitative nature of the temperature dependence changes dramatically with solvent.

Vibrational lifetimes in dense media are dominated by nonradiative decay. Dynamic intermolecular interactions of the solute's mode with the solvent produce fluctuating forces. These fluctuating forces are responsible for vibrational relaxation. Therefore, vibrational relaxation is highly dependent on the nature of the solute-solvent interactions. The fluctuating forces are frequently described in terms of the force-force correlation function. The vibrational lifetime is related to the Fourier transform of the force-force correlation function at the frequency of the relaxing mode.<sup>1,2</sup>

Vibrational relaxation can have a complicated and intertwined dependence on temperature and density. For this reason, supercritical fluids (SCFs) are useful media for the study of vibrational relaxation since the temperature and density can be controlled independently. In addition, the temperature and density dependence of vibrational relaxation can serve as a sensitive probe of solute-solvent interactions in supercritical fluids. Prior experiments on  $\text{W}(\text{CO})_6$  in supercritical ethane, carbon dioxide, and fluoroform showed unprecedented behavior of the vibrational lifetime in the vicinity of

the critical point.<sup>3,4</sup> By performing experiments along isotherms, the lifetime as a function of density at fixed temperature was measured. In general, vibrational lifetimes decreased monotonically with density. However, within a few degrees of the critical point the lifetime is density independent, or nearly so, over a substantial range in density surrounding the critical density,  $\rho_c$ . This behavior is observed in ethane, carbon dioxide, and fluoroform. A theoretical treatment of vibrational relaxation in SCFs near the critical point was developed which uses a hydrodynamic/thermodynamic approach for the calculation of the force-force correlation function.<sup>5</sup> The method permits the inclusion of critical scaling of the solvent's physical properties near the critical point. The theoretical results show a region of density independent vibrational relaxation around the critical point arising from the interplay of the critical scaling of various parameters. One property unique to the critical region is a long correlation length for local density fluctuations. These involve regions of high and low density relative to the average. The high density regions that occur even for a pure supercritical fluid have been referred to as "density enhancements." The lack of density dependence does not arise from local density enhancements caused by strong attractive solute/solvent interactions. Recently, Troe and co-workers examined multilevel vibrational relaxation of highly vibrationally excited azulene following electronic excitation and noted some evidence of a density independent region along an isotherm near the critical temperature of propane.<sup>6</sup>

The temperature dependence of the vibrational lifetime of the CO  $T_{1u}$  of  $\text{W}(\text{CO})_6$  in supercritical ethane at a constant density equal to  $\rho_c$  displays remarkable behavior. Beginning two degrees above the critical temperature, as the temperature is increased, the lifetime becomes longer. It in-

<sup>a)</sup>Permanent address: Inorganic and Physical Chemistry Department, Indian Institute of Science, Bangalore-560034, India.

<sup>b)</sup>Author to whom correspondence should be addressed.

creases with temperature until well above the critical temperature ( $\sim T_c + 70$  K) before turning around and decreasing with further increases in temperature. This behavior is contrary to expectation that the vibrational lifetime at fixed density should decrease monotonically with increasing temperature. However, the theory that was able to reproduce the density independent behavior also predicted the observed temperature dependence semiquantitatively.<sup>7</sup>

Troe and co-workers also examined multilevel vibrational relaxation of highly vibrationally excited ground state azulene for densities and temperatures far from the critical point.<sup>6</sup> The results were explained in the context of a binary collision model. An earlier report by Harris *et al.* described the temperature dependence of multilevel vibrational relaxation in the highly vibrationally excited ground electronic state of  $I_2$  following electronic excitation of  $I_2$  dissolved in supercritical Xe far from the critical point.<sup>8</sup> The data were explained, with reasonable success, by isolated binary collision models.<sup>8,9</sup> Using a semiclassical theory, Egorov and Skinner<sup>10</sup> produced very good agreement with the  $I_2$  data when a particular ansatz for the force-force correlation function was used. The binary collision models are not useful near a critical point. It is not yet clear if the Egorov-Skinner theory is accurate near the critical point.

Here, the previous temperature dependent experiments on  $W(CO)_6$  at constant density are extended to a range of densities in ethane and to fluoroform and  $CO_2$ . When the  $W(CO)_6$  temperature dependent vibrational lifetime is examined in ethane at densities away from  $\rho_c$ , near quantitative agreement with theory is achieved at some densities. However, when the temperature dependent lifetime of the  $T_{1u}$  mode of  $W(CO)_6$  is measured in supercritical  $CO_2$  at  $\rho_c$ , the "inverted" temperature dependence seen in ethane is not observed. In fluoroform, a weakly inverted region is observed. The appearance of an inverted region seems to be correlated with the effectiveness of the solute-solvent coupling in inducing vibrational relaxation.

## II. EXPERIMENT

The details of the experiment have been described elsewhere.<sup>4,11</sup> Briefly, cavity dumped pulses from a Q-switched, mode locked, Nd:YAG laser are doubled and used as the pump pulses in a  $LiIO_3$  OPA. The YAG laser is also output coupled. The doubled pulse train synchronously pumps a cavity dumped dye laser (Rhodamine 610 in ethanol). The dye laser pulse is double passed amplified. The amplified dye pulse provides the signal pulse for the OPA. The typical OPA output at  $\sim 5 \mu m$  is  $1.5 \mu J$  in a 40 ps pulse. The exact frequency of the IR is tuned to the peak of the  $\nu = 0 \rightarrow 1$  CO  $T_{1u}$  mode absorption of the solute,  $W(CO)_6$ . The frequency, which depends on the temperature and density of the solvent, is  $\sim 1980 \text{ cm}^{-1}$ .

The sample is contained in a high pressure, high temperature cell constructed from Monel 400 and sealed with sapphire windows. The temperature and pressure are accurately monitored and controlled. Samples are prepared by inserting a minute quantity of pure  $W(CO)_6$  into the cell and then purging the system of air with the solvent gas. The cell is then pressurized and the absorbance of the solute is mea-

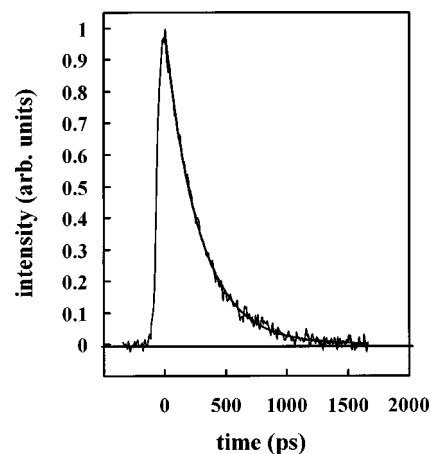


FIG. 1. Pump-probe data on the asymmetric CO stretching mode of  $W(CO)_6$  in supercritical ethane ( $1990 \text{ cm}^{-1}$ ) at the critical density and 38 K above  $T_c$ . The heavy line is a fit to a single exponential. The lifetime  $T_1 = 278$  ps. Similar quality data were taken at other temperatures and densities in ethane, as well as in carbon dioxide and fluoroform.

sured with a FTIR spectrometer. The IR beam from the FTIR spectrometer is taken out of the instrument, passed through the sample cell, and into an external IR detector. Optical densities of  $\sim 1$  were ideal, though experiments at low densities were typically done with much smaller ( $\sim 0.3$ ) absorbances. These optical densities correspond to solute concentrations of roughly  $10^{-5} \text{ mol/l}$ . It was found that absorbances substantially greater than 1 can produce anomalous results. Care was taken to assure that at each temperature and density, the absorbance was not too great.

Pump-probe experiments are carried out in a counter-propagating manner in which the pump and probe pulses are collinear but enter from opposite sides of the cell. The probe intensity is measured on an InSb detector and compared to the signal from a reference detector. The decays were fit by single exponentials, which resulted in excellent residuals in almost all cases.<sup>23</sup> Occasionally, when the energy of the IR was about  $2 \mu J$  or more, noticeable up-pumping to higher vibrational levels occurred and resulted in a poor single exponential fit. In this case, filters were used in the pump beam and single exponential decays were recovered.

## III. RESULTS AND DISCUSSION

Figure 1 displays pump-probe vibrational lifetime data taken on the CO  $T_{1u}$  mode of  $W(CO)_6$  in ethane at  $T = 343$  K and  $\rho = 6.87 \text{ mol/l}$  ( $T_c = 305$  K;  $\rho_c = 6.87 \text{ mol/l}$ ). An exponential fit is also shown. The decay time is 278 ps. Data such as this were acquired at several densities as a function of temperature. Figure 2 shows the temperature dependence at  $\rho_c$ .<sup>23</sup> The lowest temperature point is 2 K above  $T_c$  and the temperature dependence extends to  $T \approx 500$  K. As the temperature is raised above the critical point, the lifetime lengthens, finally peaking well above  $T_c$ . Following the peak, the lifetime decreases with further increases in temperature. The peak occurs at  $\sim 373$  K, which is  $\sim 70$  K above  $T_c$ . The right-hand scale on the figure is the reduced lifetime, which is the lifetime divided by the lifetime at a reference temperature,  $T_{rf}$ . In this plot, the reduced lifetime scale

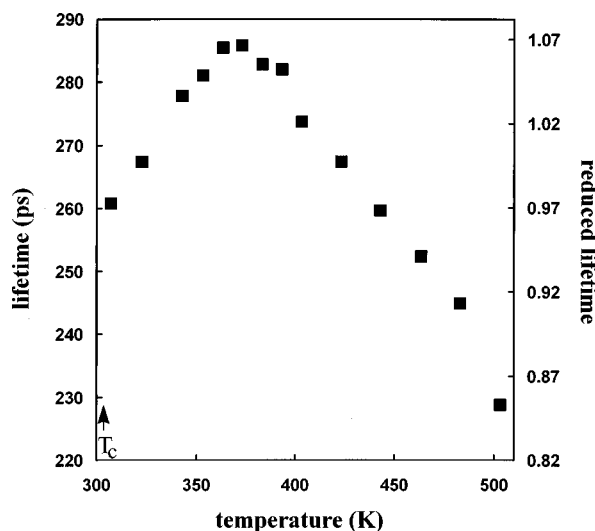


FIG. 2.  $T_1$  data for the asymmetric CO stretching mode of  $W(CO)_6$  in supercritical ethane as a function of temperature at constant density. The density is the critical density,  $\rho_c = 6.87 \text{ mol/l}$ . The left-hand ordinate gives the lifetimes in ps and the right-hand ordinate is the reduced lifetime, i.e., the lifetime normalized with respect to the lifetime at a reference temperature,  $T_{\text{ref}} = 323 \text{ K}$ . The data display a region of inverted temperature dependence in which the lifetime increases as the temperature increases.

is calculated using  $T_{\text{ref}} = 323 \text{ K}$ . The reduced lifetime facilitates comparison with the theoretical calculations presented below.

While the increase in the lifetime with temperature shown in Fig. 2 is not large,  $\sim 10\%$ , it nonetheless shows a dramatic deviation from the behavior that would be expected as the temperature is increased at constant density. In the simplest example, one may consider a system dominated by independent binary collisions. As the temperature is increased at a fixed density, the collision frequency will increase and thus lead to faster energy transfer. Also, the probability that a collision will induce energy transfer increases with temperature since the collisions will occur at higher velocities and thus with more force. Harris found this reduction of the lifetime with temperature in the  $I_2/\text{Xe}$  system far from the Xe critical point.<sup>8</sup>

At a density of  $6.87 \text{ mol/l}$ , the independent binary collision model may not be valid, particularly for a polyatomic solute in a polyatomic solvent. However, theories for vibrational relaxation in liquids or crystals also predict that the lifetime will decrease as the temperature increases at constant density.<sup>2,10,12</sup> The rate of vibrational relaxation,  $K$ , of the initially excited mode can be described by Fermi's Golden Rule,<sup>2,12,13</sup>

$$K = \frac{2\pi}{\hbar} \sum_{r,r'} \rho_{r,r'} |\langle \sigma', r' | V | \sigma, r \rangle|^2. \quad (1)$$

In Eq. (1),  $\sigma$  and  $\sigma'$  denote the initial and final state of the initially excited vibration (the  $T_{1u}$  mode in this case), while  $r$  and  $r'$  refer to the receiving (or reservoir) modes. The reservoir includes all intra- and intermolecular modes of the solvent as well as modes of the solute other than the relaxing mode. The ket  $|\sigma, r\rangle$  is the initial state, described by thermal occupation numbers of the various modes of the system, in

addition to unity occupation of the state initially excited by the IR pump. The bra  $\langle \sigma', r' |$  is the final state with the initially populated state having occupation number 0 after relaxation and other states having increased (or decreased) occupation numbers.  $\rho$  is the density of states of the reservoir modes for the relaxation step. The summation in Eq. (1) denotes the fact that the true relaxation rate is a sum over contributions from all possible pathways;<sup>12</sup> however, in the following discussion we will describe relaxation through a single anharmonic path involving one phonon.

In Eq. (1),  $V$  is the potential that describes the system-reservoir interaction.<sup>12</sup>  $V^{(i)}$  is the  $i$ th matrix element that describes the interactions which couple  $i$  modes. The anharmonic terms,  $i \geq 3$ , govern relaxation processes involving the coupling of multiple vibrational modes. Given the vibrational energies of the solutes and the solvents, the relaxation of the initially excited mode results in the excitation of at least two other vibrations and a phonon. Here phonon is used as a general term to mean a mode of the low frequency continuum of the solvent. In a crystal, the continuum is composed of true phonons. In a liquid or SCF the continuum may be thought of in terms of instantaneous normal modes (INM).<sup>14,15</sup> For such a process, the anharmonic coupling matrix element is at least fourth order, or quartic. For the following discussion, a single quartic relaxation pathway is discussed, but the conclusions are quite general.

The quartic anharmonic matrix element  $\langle V^{(4)} \rangle$  contains the magnitude of the quartic anharmonic coupling term,  $|V^{(4)}|$ , and combinations of raising and lowering operators that describe the anharmonic relaxation step.<sup>12,16</sup> If the operator  $a_1$  annihilates the initially excited vibration and the operators  $b$  and  $b^+$  describe the change in the reservoir modes  $A, B$ , and the phonon, then the interaction is described by

$$a_1 (b_A + b_A^+) (b_B + b_B^+) (b_{\text{ph}} + b_{\text{ph}}^+). \quad (2)$$

This interaction leads to seven possible quartic relaxation pathways,<sup>12</sup> some of which are unphysical. The relaxation pathway being considered, a simple cascade process in which the energy relaxes only to lower energy modes, is described by one term arising from Eq. (2),  $a_1 b_A^+ b_B^+ b_{\text{ph}}^+$ , i.e., the initially excited vibration is annihilated, and each of the modes  $A, B$ , and  $\text{ph}$  are excited. Once substituted into Eq. (1), a raising operator brings out a factor of  $\sqrt{n+1}$  and a lowering operator brings out a factor of  $\sqrt{n}$ , where  $n$  is the occupation number of the particular mode involved in the 4th order process. Since the initially excited mode has  $n=1$ , the  $a_1$  brings out a factor of unity. This allows Eq. (1) to be written as

$$K = \frac{2\pi}{\hbar} \rho_{\text{ph}} |\langle V^{(4)} \rangle|^2 (n_A + 1)(n_B + 1)(n_{\text{ph}} + 1), \quad (3)$$

where  $n$  is the thermally averaged occupation number,

$$n_i = (\exp(\hbar \omega_i / kT) - 1)^{-1}. \quad (4)$$

$\omega_i$  is the frequency of the vibrational or phonon mode. Taking  $\rho_{\text{ph}} = \langle \rho(\omega_i) \rangle$ , the "phonon" density of states is given by the ensemble averaged density of INM.

If the reservoir modes are high frequency ( $\hbar\omega \gg kT$  and, therefore,  $n=0$ ), such as the discrete vibrational modes of the solute and solvent, Eq. (3) is

$$K = \frac{2\pi}{\hbar} \rho_{\text{ph}} |\langle V^{(4)} \rangle|^2 (n_{\text{ph}} + 1). \quad (5)$$

Although the discussion of the derivation of this relaxation rate expression has been qualitative, the same results can be shown rigorously.<sup>12</sup> In general, the expression for the relaxation rate along a given one-phonon,  $i$ th order anharmonic pathway is given by the product of the phonon density of states, the magnitude of the anharmonic coupling matrix element squared, and occupation number factors for the receiving modes. If a reservoir mode is created in the relaxation step, it contributes a factor of  $(n+1)$ , whereas if it is annihilated, it contributes a factor of  $n$ . This is a simple, yet rigorous, method for describing even complex relaxation pathways.

Considering only the occupation number in Eq. (5),  $K$  should become larger and the observed decay times should become shorter as the temperature is increased. If more than one thermally occupied phonon were involved in the relaxation pathway or if a vibrational occupation number changes significantly, the temperature dependence would be even steeper. If the phonon occupation number is the only factor responsible for the temperature dependence, then for  $\hbar\omega \ll kT$ ,  $K$  would increase linearly with temperature. For  $\hbar\omega \gg kT$ ,  $K$  goes as  $\exp(-\hbar\omega/kT)$  if a phonon is annihilated as part of the relaxation process, and  $K$  goes as  $1 + \exp(-\hbar\omega/kT)$  if a phonon is created. In either limit and for intermediate situations, the temperature dependence of the occupation number(s) will always yield a decrease in the vibrational lifetime with increasing temperature. Only near  $T \approx 0$  K (only phonon emission processes are possible) where  $1 > n_{\text{ph}}$ , will the temperature dependence vanish, and the vibrational lifetime will become temperature independent. Above  $T \approx 0$  K, an inverted temperature dependence cannot be explained by considering occupation numbers, regardless of the pathways or number of modes involved.<sup>12</sup>

In a study of the temperature dependent vibrational lifetime of the  $T_{1u}$  mode of  $\text{W}(\text{CO})_6$  in liquid  $\text{CHCl}_3$ , the lifetime was observed to increase (inverted temperature dependence) in going from the melting point to the boiling point of the solvent.<sup>16</sup> However, as the temperature is increased, the density of the liquid decreases. In Eq. (5), both the density of states and the magnitude of the anharmonic coupling matrix element can be density dependent. Theoretical analysis indicated that the inverted temperature dependence was due to a reduction in the magnitude of the anharmonic coupling matrix element as the density decreased.<sup>14</sup> However, in the current study, the density is fixed. Therefore, the inverted temperature dependence cannot arise from a density dependence of the intermolecular interactions as it can in a liquid.

While the Golden Rule formalism outlined above<sup>12</sup> is useful for enumerating vibrational relaxation pathways and gaining insights into possible sources of temperature dependence, it does not provide a method for including detailed properties of a liquid or SCF solvent into the calculation of vibrational relaxation. In a SCF in the vicinity of the critical

point, it is particularly important to use a method that can incorporate the solvent properties that change rapidly with temperature and density, such as the isothermal compressibility and the thermal diffusivity. Cherayil and Fayer developed a free energy density functional theory of the force-force correlation function. The usefulness of the theory is that the force-force correlation function can be evaluated in terms of known thermodynamic and hydrodynamic properties of the solvent. The theory starts with the standard relationship between the vibrational lifetime,  $T_1$ , and a classical description of the force-force correlation function,

$$T_1^{-1} = \frac{\beta}{m} \int_0^\infty dt \langle F(t)F(0) \rangle_{\text{cl}} \cos(\omega t). \quad (6)$$

$\beta$  is  $1/k_B T$ , where  $k_B$  is Boltzmann's constant,  $m$  is the reduced mass of the oscillator, and  $\omega$  is the oscillator frequency. The theoretical analysis yields the following expression:

$$T_1^{-1} \propto T \int_0^\infty dt \cos(\omega t) \int d\mathbf{k} k^2 |\hat{C}_{21}(\mathbf{k})|^2 \hat{S}_1(\mathbf{k}, t). \quad (7)$$

$\hat{C}_{21}(\mathbf{k})$  is the Fourier transform of the direct correlation function<sup>17</sup> and  $\hat{S}_1(\mathbf{k}, t)$  is the dynamic structure factor.<sup>18</sup> Equation (7) was evaluated for different regimes of density and temperature, very near the critical point and farther from the critical point. In the experiments presented here, the temperatures are sufficiently far above the critical temperature that the noncritical region version of the theory is appropriate.

When Eq. (7) is evaluated for the noncritical region using a variety of approximations to yield an analytical expression,<sup>5</sup>  $1/T_1$  has the form

$$\frac{1}{T_1} \propto T^2 \rho_1 \frac{\kappa_T}{\kappa_T^0} \hat{C}_{12}(0)^2 \Lambda^3 \left( Q_A - \frac{1}{\gamma} Q_A + \frac{1}{\gamma} Q_B \right), \quad (8)$$

where  $\rho_1$  is the number density of the solvent,  $\kappa_T$  is its isothermal compressibility,  $\kappa_T^0$  is the isothermal compressibility of the ideal gas, and  $\Lambda$  is a cutoff on high momenta. It is chosen to meet the condition for the noncritical regime,  $\Lambda \xi < 1$ . The results of the calculations are not sensitive to  $\Lambda$ , and  $\Lambda$  is set equal to  $2 \times 10^{-8} \text{ m}^{-1}$ .  $\gamma \equiv C_p/C_v$  is the ratio of specific heats.  $Q_A$  is a function of the correlation length of density fluctuations  $\xi$  and of the thermal diffusivity  $D_T$ ; it is defined as

$$Q_A = \frac{\bar{\Lambda}^2}{D_T(1 + \omega_1^2)} [R_1 + R_2 - R_3], \quad (9a)$$

where  $\bar{\Lambda} = \Lambda \xi$ ,  $\omega_1 = \omega \xi^2/D_T$ , and

$$R_1 = 1 - \frac{5}{3\bar{\Lambda}^2} \left[ 1 + \frac{3}{\bar{\Lambda}^2} \left\{ \frac{\tan^{-1} \bar{\Lambda}}{\bar{\Lambda}} - 1 \right\} \right], \quad (9b)$$

$$R_2 = \frac{5}{3\bar{\Lambda}^2} \left[ 1 + \frac{3}{4\sqrt{2}} \omega_1^{3/2} \{ \ln S_1 - 2 \tan^{-1} S_2 \} \right], \quad (9c)$$

$$R_3 = 1 - 5\omega_1^2 + \frac{5}{4\sqrt{2}} \omega_1^{5/2} [ \ln S_1 + 2 \tan^{-1} S_2 ], \quad (9d)$$

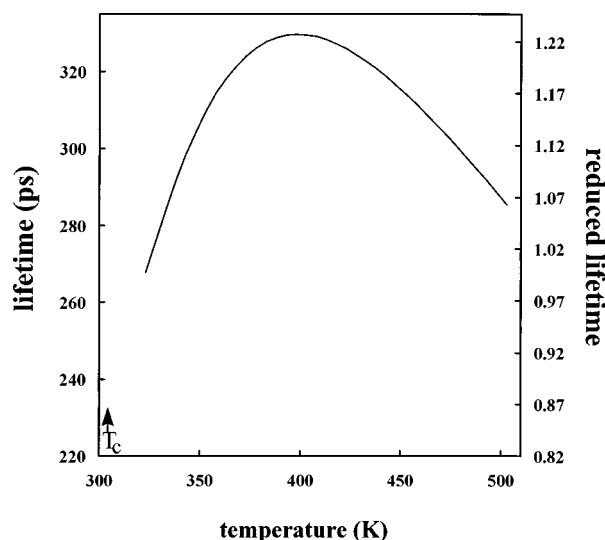


FIG. 3. Calculated vibrational lifetimes of the asymmetric CO stretching mode of  $W(CO)_6$  in supercritical ethane at the critical density. There are no adjustable parameters other than the vibrational lifetime is normalized with respect to the lifetime at  $T_{rf}=323$  K. The calculations reproduced the data semiquantitatively, predicting an inverted temperature dependence.

with  $\omega_2 = \omega/\Lambda^2 D_T$ . The functions  $S_1$  and  $S_2$  are defined by  $S_1 = (1 + \sqrt{2\omega_2 + \omega_2}) / (1 - \sqrt{2\omega_2 + \omega_2})$ , and  $S_2 = \sqrt{2\omega_2} / (\omega_2 - 1)$ .  $Q_B$  is identical to  $Q_A$  except that  $D_T$  is replaced everywhere by the sound attenuation constant  $\Gamma$ , which is given by  $\Gamma = D_T(\gamma - 1) + (4\eta_s/3 + \eta_b)/\rho_m$ , where  $\eta_s$  is the shear viscosity,  $\eta_b$  is the bulk viscosity, and  $\rho_m$  is the mass density. In deriving Eqs. (9a)–(9d), the limit  $c_s k \ll \omega$  was assumed to hold,  $c_s$  being the adiabatic sound velocity. The thermodynamic quantities in these relations are obtained from the NIST equations of state for ethane and  $CO_2$ .<sup>19</sup>

Figure 3 shows the results of calculations using Eq. (8) for the experimental situation of the data in Fig. 2. The calculations are displayed in terms of the reduced lifetime. The calculations begin 20 K above  $T_c$ , the beginning of the region in which the noncritical form of the theory given by Eq. (8) is valid. Other than setting the reduced lifetime equal to 1 at  $T_{rf}=323$  K, there are no adjustable parameters in the calculation. All of the necessary parameters in Eq. (8), which characterize the solvent, are known. The most important feature of the calculation is that it displays the inverted temperature dependence seen in the data. The peak of the curve is at  $\sim 395$  K, which compares favorably with the experimental peak at  $\sim 375$  K. However, the magnitude of the peak, 1.23, is substantially greater than the peak in the experimental data of 1.06. While the calculation misses the magnitude of the peak, the slope of the calculated temperature dependence in the high temperature region matches the data quite well. This can be seen in Fig. 4 in which the data and the calculation are shown but with the reference temperature,  $T_{rf}$ , for the reduced lifetime equal to 423 K.

Figure 5 displays vibrational lifetime temperature dependence data<sup>23</sup> at several fixed densities above and below  $\rho_c$  in ethane solvent along with theoretical calculations. In Fig. 5,  $T_{rf}=323$  K, as in Fig. 3. Figure 5(a) is for the density  $\rho=5$  mol/l. There are no adjustable parameters in the calculation aside from setting the reduced concentration to 1 in both the

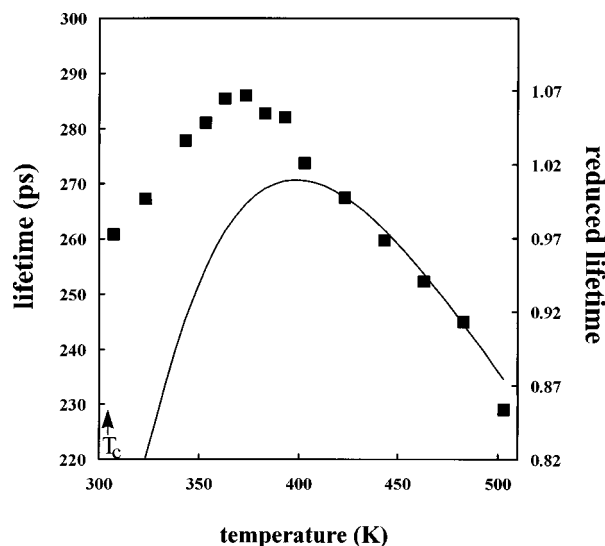


FIG. 4. The data of Fig. 2 and calculations with  $T_{rf}=423$  K. The theory does a reasonable job of calculating the temperature dependence at temperatures well above the critical temperature, i.e., past the region of the inverted temperature dependence.

experiment and the calculation at  $T_{rf}$ . Like the data at  $\rho_c$ , the data at  $\rho=5$  mol/l show a pronounced region of inverted temperature dependence. The agreement between theory and experiment is very good, much better than for  $\rho_c$ . The peak location and magnitude are correct within experimental error. The calculated peak appears to be slightly too narrow as it turns over too soon. The inset shows that the slope at temperatures well above the inverted regime is predicted quite accurately. Figure 5(b) illustrates data measured at  $\rho=10$  mol/l. The data still show an inverted region, but the peak is only  $\sim 40$  K above  $T_c$  and the amplitude at the maximum less than at the lower densities. The agreement with the calculations is much worse than at the lower density of Fig. 5(a). The calculations do predict a decrease in the amplitude and temperature of the peak compared to the data at  $\rho_c$  but still heavily overestimate the extent of the inverted region. The inset shows that the calculations do provide very good agreement with the slope of the temperature dependence for temperatures well above the inverted regime. Figure 5(c) displays data at  $\rho=12$  mol/l. In the region of applicability of Eq. (8), the agreement is reasonably good. However, the calculation shows a very shallow peak which is not evident in the data. The point 2 K above  $T_c$  does not fall on the calculated trend, but this point may be outside the range of validity of Eq. (8). For the data at this density, the error bars are  $\pm 5$  ps. With these error bars, it is possible to draw a straight line through all of the data. Unlike the data in Figs. 3 and 5(a), it is unclear if the data in Fig. 5(c) display an anomalous temperature dependence.

Figure 6(a) shows temperature dependent lifetime data for the  $CO T_{1u}$  mode of  $W(CO)_6$  in supercritical  $CO_2$  at the  $CO_2$  critical density,  $\rho_c=10.6$  mol/l. Figure 6(b) shows this same data along with the data for the ethane solvent (Fig. 3) at the ethane  $\rho_c$  as a reduced lifetime plot to facilitate comparison. Clearly, the lifetime data with  $CO_2$  solvent and with ethane solvent are very different, although both experiments

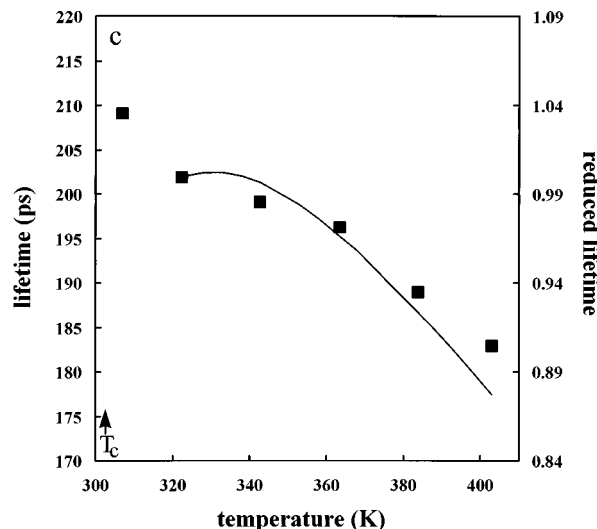
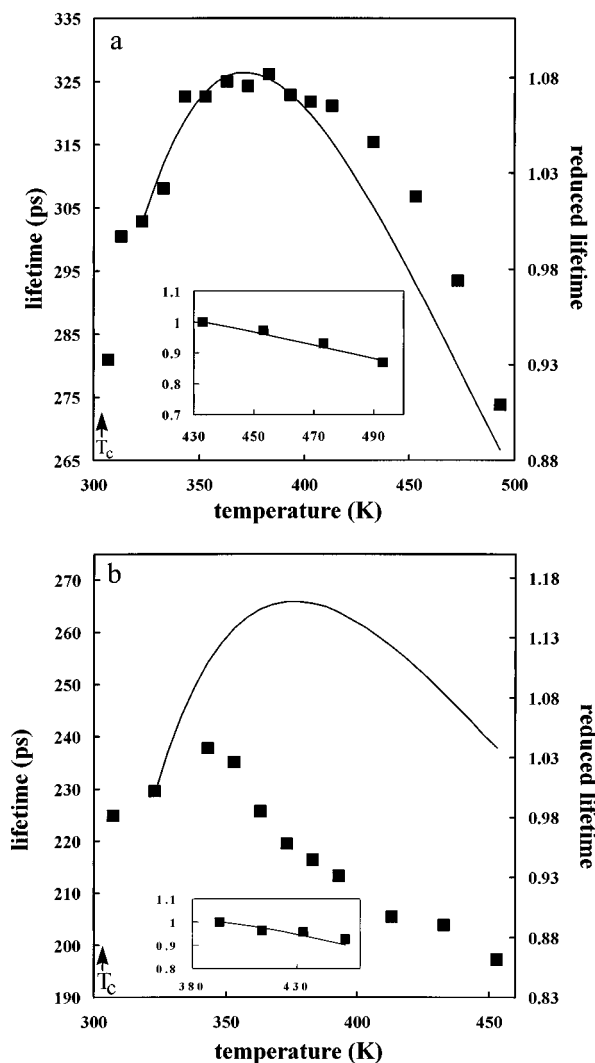


FIG. 5. Experimental and theoretical vibrational lifetime data for the asymmetric CO stretching mode of  $W(CO)_6$  in supercritical ethane as a function of temperature at several densities. (a) Data for  $\rho=5.0$  mol/l. The data display an inverted temperature dependence. The extent to which the lifetime increases from its value near the critical point is larger than at the critical density (see Fig. 2). The theory nearly quantitatively reproduces the vibrational lifetime data. The inset shows data and calculations with  $T_{ref}=403$  K. The theory accurately reproduces the slope of the lifetime temperature dependence at high temperatures. (b) Data at  $\rho=10.0$  mol/l. The region in which the lifetime increases with temperature above  $T_c$  still persists but to a much smaller degree. The agreement between the theory and data is much worse. The inset shows data and calculations with  $T_{ref}=393$  K. The theory accurately reproduces the slope of the lifetime temperature dependence at high temperatures. (c) Data at  $\rho=12.0$  mol/l. There is no apparent inverted region. In fact the data may fall on a straight line. The theory with  $T_{ref}=323$  K reproduces the data reasonably well, but still shows a suggestion of an inverted region.

were performed at  $\rho_c$ . The  $CO_2$  solvent data displays a negligible inverted regime. Only the point near  $T_c$  may be anomalously fast, and this point is very close to the critical point. Figure 7 shows theoretical calculation of the reduced lifetimes for both  $CO_2$  (bottom curve) and ethane (top curve) solvents. The calculation and the data were matched at  $T_{ref}=323$  K. The calculations for the  $CO_2$  solvent do not reproduce the qualitative behavior of the data. The calculations do show that the peak height is lower and shifted to lower temperature in comparison to the calculations with ethane as the solvent. As noted in comparing the calculations in Fig. 3 to the data in Fig. 2, the calculated peak overshoots the data by a considerable amount. It is possible that an improved calculation that more accurately reproduced the ethane results would be qualitatively consistent with the data in  $CO_2$  solvent. Independent of the ability of the theory to reproduce the data, an important point is that the temperature dependent vibrational relaxation of the same solute in two different SCF solvents at  $\rho_c$  is very different, not only in the absolute rates, but also in the functional form of the temperature dependence.

The data shown in Fig. 6 raise an interesting question. Is the behavior seen in the ethane solvent an exception to what might be considered the normal temperature dependence ob-

served in  $CO_2$ ? The density dependence of the vibrational lifetime at constant temperature for  $T$  close to  $T_c$  in the two solvents is very similar. In both solvents, the vibrational lifetimes display a density independent region around  $\rho_c$ . This behavior is also observed when fluoroform is the solvent. Figure 8 shows the vibrational lifetime of the CO  $T_{1u}$  mode of  $W(CO)_6$  as a function of temperature in fluoroform at its critical density ( $\rho_c=7.56$  mol/l). These data show a broad, very shallow peak. The peak is  $\sim 35$  K above  $T_c$  ( $T_c=299$  K). The behavior of the lifetime in fluoroform is intermediate between that in ethane, which shows a pronounced peak, and that in  $CO_2$ , which shows essentially no peak. Comparison of the temperature dependent vibrational lifetimes in the three solvents suggests that there is a range of behaviors depending on the solvent, from a significant inverted temperature dependence to no inverted temperature dependence.

In scanning the ranges of temperatures in the three solvents, the experiments begin 2 K above the critical points of the solvents. The critical points are only a few degrees apart. Therefore, the ranges of temperatures are essentially identical, and differences in temperatures cannot account for the differences in the temperature dependence of the vibrational lifetimes observed in the three solvents. There are other

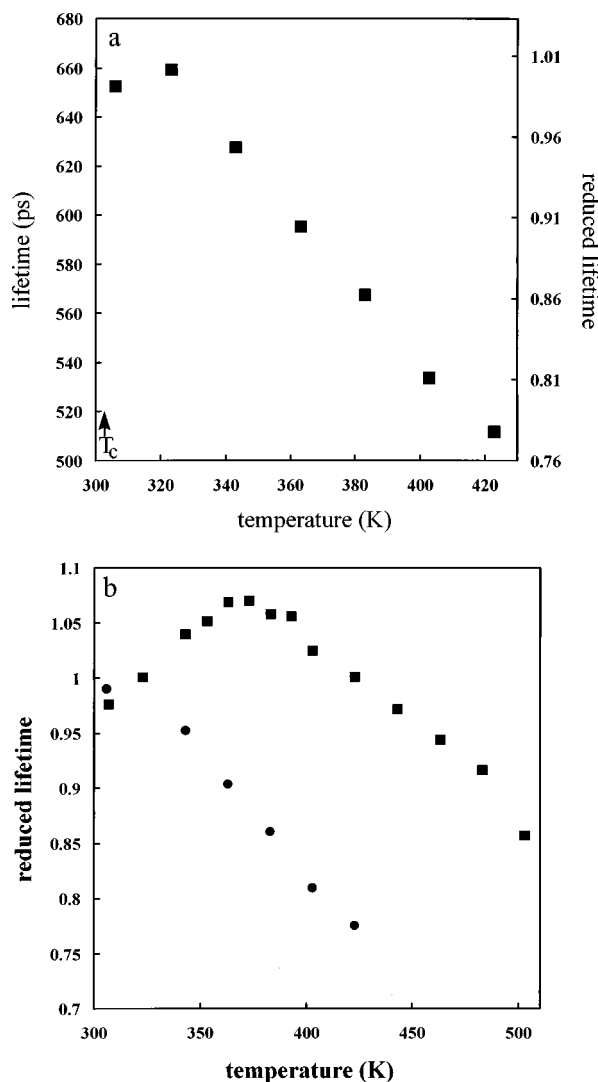


FIG. 6. Experimental vibrational lifetime data for the asymmetric CO stretching mode of  $W(CO)_6$  in supercritical  $CO_2$  as a function of temperature at constant density. The density is the critical density,  $\rho_c = 10.6 \text{ mol/l}$ . Unlike the data with ethane as the solvent, the data display a negligible inverted temperature dependence. (b) A comparison of the reduced vibrational lifetime data for  $CO_2$  (circles) and ethane (squares) solvents.

trends in the lifetimes when the solvent is changed that are noteworthy. At  $\rho = 8 \text{ mol/l}$  and 2 K above their respective critical points, the vibrational lifetimes in ethane, fluoroform, and  $CO_2$  are 240 ps, 480 ps, and 660 ps. At 2 K above  $T_c$ ,  $\rho = 8 \text{ mol/l}$  is within the range of densities for each solvent in which the lifetime is virtually density independent, so the fact that this density varies a different amount from  $\rho_c$  does not affect the comparison. Thus, with the same density, the same increment of temperature above the critical point, and virtually the same absolute temperature, the vibrational lifetime varies substantially with solvent.

A decrease in the lifetime for the same vibrational mode when the solvent is changed indicates an increased coupling between the solute mode and the solvent. At room temperature in liquid  $CCl_4$ , the CO  $T_{1u}$  mode of  $W(CO)_6$  has a lifetime of 700 ps, while in liquid  $CHCl_3$  at the same temperature, the lifetime is reduced to 350 ps.<sup>16</sup> Calculations of

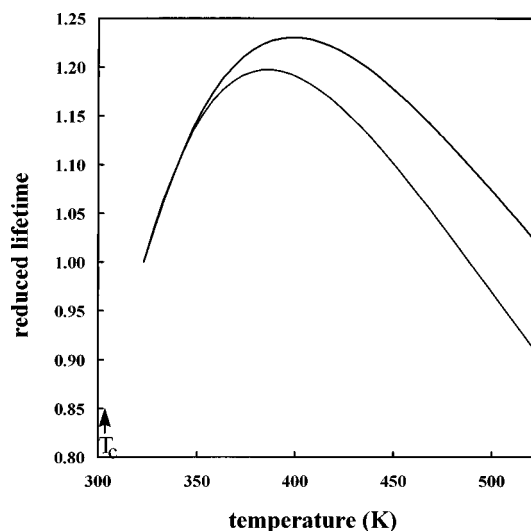


FIG. 7. Theoretically calculated temperature dependent vibrational lifetimes for the asymmetric CO stretching mode of  $W(CO)_6$  in supercritical ethane (top curve) and carbon dioxide (bottom curve) at their critical densities. The theory predicts the presence of significant regions of inverted temperature dependence in both ethane and carbon dioxide. The calculations show the peak height is greater and the peak position is at higher temperature in ethane.

the low frequency continuum density of states show that they are approximately the same in the two solvents.<sup>14</sup> It has been suggested<sup>12,16</sup> that the difference in the lifetimes arise from differences in the relaxation pathways involving high frequency modes of the solvent.  $CHCl_3$  has a H-C-Cl bend at  $1220 \text{ cm}^{-1}$ . This makes it possible for the  $\sim 2000 \text{ cm}^{-1}$   $W(CO)_6$  mode to relax via a quartic anharmonic process as described by Eq. (3). The initial vibration is annihilated and a CH bend and another low frequency mode of the solvent or solute are created. To have energy conservation, a low frequency phonon mode of the continuum ( $\leq 200 \text{ cm}^{-1}$ ) is also created. Because  $CCl_4$  has only low frequency modes, a fifth

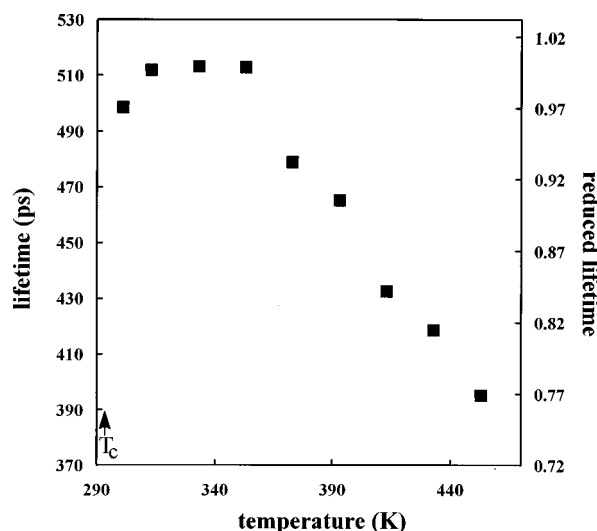


FIG. 8. Experimental vibrational lifetime data for the asymmetric CO stretching mode of  $W(CO)_6$  in supercritical fluoroform at the critical density ( $7.56 \text{ mol/l}$ ). The data display an inverted temperature dependence that is intermediate between that observed in ethane solvent (Fig. 2) and  $CO_2$  solvent (Fig. 6).

order process is required for the relaxation, and the decay time is substantially longer.<sup>12,16</sup> Furthermore, in liquid 2-methylpentane, there are a very large number of C–H bending modes in the range of 1300–1400  $\text{cm}^{-1}$ , and the  $\text{W}(\text{CO})_6$   $T_{1u}$  mode has a much shorter lifetime of 145 ps.<sup>20</sup> Apparently, the C–H bending modes are important in the relaxation of the asymmetric stretching mode of  $\text{W}(\text{CO})_6$ .

Given the above, the 480 ps lifetime observed in fluoroform at 8 mol/l is consistent with the observation in liquid chloroform. The lifetime in chloroform is shorter but it is a liquid. The lifetime in ethane is even faster, akin to the decrease in lifetime observed in going from liquid chloroform to liquid 2-methylpentane. In both cases, i.e., fluoroform to ethane and chloroform to 2-methyl pentane, there is a large increase in the number of C–H bending modes available to participate in the vibrational relaxation. When  $\text{CO}_2$  is the SCF solvent, the longest lifetime is observed. Like  $\text{CCl}_4$ ,  $\text{CO}_2$  has no C–H bends. However,  $\text{CO}_2$  does have the symmetric O–C–O stretch at 1388  $\text{cm}^{-1}$ . If the energy of the available modes was the only determining factor, then it would be expected that relaxation in  $\text{CO}_2$  would be more similar to relaxation in fluoroform. The fact that the lifetime is substantially slower in  $\text{CO}_2$  suggests that the anharmonic coupling matrix element [e.g., see Eq. (3)] involving the  $\text{CO}_2$  symmetric stretch and the asymmetric CO stretching mode of  $\text{W}(\text{CO})_6$  is small.

From the lifetimes in the three solvents, it is clear that the order of the strength of the interaction between the CO  $T_{1u}$  mode of  $\text{W}(\text{CO})_6$  and the solvent is ethane, fluoroform,  $\text{CO}_2$  (strongest coupling to weakest). Another indication of this order of coupling is the change in the lifetime with density. At  $\rho=2$  mol/l and 2 K above their respective critical points, the vibrational lifetimes in ethane, fluoroform, and  $\text{CO}_2$  are 515 ps, 770 ps, and 920 ps. The ratio,  $R$ , of the lifetime at 2 mol/l to the lifetime at 8 mol/l in ethane, fluoroform, and  $\text{CO}_2$  is 2.15, 1.60, and 1.39, respectively. The sensitivity of the lifetime to density is greatest in ethane, less in fluoroform, and least in  $\text{CO}_2$ .

The nature of the temperature dependence at fixed density,  $\rho_c$ , in the three solvents appears to be correlated with the strength of the solute  $\text{W}(\text{CO})_6$  CO  $T_{1u}$  mode coupling to the solvent. When the coupling is relatively strong, as in ethane, the temperature dependence has a significant inverted region and a significant peak in the plot of lifetime vs temperature (Fig. 2). When the coupling is moderate, as in fluoroform, there is a less pronounced peak and a narrower inverted region (Fig. 8). When the coupling is weak, as in  $\text{CO}_2$ , there is no significant peak [Fig. 6(a)]. While the thermodynamic/hydrodynamic theory captures the behavior in ethane, at least semiquantitatively, it does not in  $\text{CO}_2$ . (Sufficient thermodynamic data are not available in the literature to perform the calculations for fluoroform). As suggested above, the shorter lifetime observed in ethane compared to  $\text{CO}_2$  can result from more efficient coupling of the initially excited  $\sim 2000$   $\text{cm}^{-1}$  solute mode to high frequency modes of the solvent. The theory does not explicitly account for vibrational relaxation into high frequency vibrational modes of the bath. If relaxation in ethane is dominated by high frequency modes of the bath, then the relaxation may

involve only one phonon. In contrast, relaxation in  $\text{CO}_2$  may require a multiphonon process, which may not be well described by the current thermodynamic/hydrodynamic theory. Regardless of the theory's ability to reproduce the data in the various solvents, it is clear that the nature of the solute–solvent interactions has a fundamental influence on the qualitative behavior of the temperature dependence of the vibrational lifetime at fixed density near the critical point.

#### IV. CONCLUDING REMARKS

The experiments presented here and the previous work on which they are based<sup>4,7</sup> are the first experiments to examine vibrational relaxation between a well defined pair of vibrational levels in SCFs in the vicinity of the critical point. The results of the experiments have revealed the complex interplay between rapidly changing macroscopic properties of SCFs near the critical point and microscopic molecular dynamics and intermolecular interactions. In three SCF solvents for  $T$  near  $T_c$ , the asymmetric CO stretching mode of  $\text{W}(\text{CO})_6$  displays essentially density independent vibrational lifetimes near  $\rho_c$ . The thermodynamic/hydrodynamic theory of vibrational relaxation,<sup>5</sup> which is capable of including the critical scaling of the important physical properties of SCFs, predicts the observed behavior. The theory, which calculates  $T_1$  by obtaining analytical expressions for the force–force correlation function, shows that the density independence (or extremely weak density dependence) comes from an interplay of rapidly changing density dependent properties which offset each other near the critical point. Recently, Tucker and co-workers<sup>21</sup> performed two dimensional simulations to obtain the force–force correlation function for a rigid diatomic in an atomic solvent. They also found  $T_1$  to be nearly density independent around  $\rho_c$ . Near the critical point, normal large fluctuations in density give rise to regions of high density. In both the analytical theory and the simulations, ensemble averages are performed over all solute environments. However, neither the analytical theory discussed here nor the simulations involved any type of local density enhancements through attractive solute/solvent interactions to produce the density independent results. In addition, experiments on asymmetric CO stretching modes of both  $\text{W}(\text{CO})_6$  and (acetylacetonato)dicarbonylrhodium(I) ( $\text{Rh}(\text{CO})_2\text{acac}$ ) found the vibrational absorption line position is density independent in a range of densities around  $\rho_c$  when  $T$  is near  $T_c$ . The analytical theory also predicts this behavior.

As shown in Figs. 2 and 5, the lifetime of the asymmetric CO stretching mode of  $\text{W}(\text{CO})_6$  in ethane as a function of temperature at fixed density at and near  $\rho_c$  displays a region of inverted temperature dependence. The vibrational lifetime increases as the temperature is increased, then turns over and decreases with further increases in temperature. This behavior occurs to a lesser extent when fluoroform is the solvent, but does not occur to any significant extent when  $\text{CO}_2$  is the solvent. While the current analytical theory is able to capture the essence of the data when ethane is the solvent, it is qualitatively incorrect when  $\text{CO}_2$  is the solvent. A new theoretical approach for calculation of vibrational lifetimes in SCFs, which is still able to account for critical phenomena through



the use of hydrodynamic and thermodynamic functions, is under development.<sup>22</sup> Preliminary results show that the new theory also predicts the region of density independence near the critical point without invoking solute/solvent clustering. Additional experiments are underway which are examining other solute molecules to determine if they also display the same temperature and density dependent behaviors of the vibrational lifetime in the neighborhood of the critical point.

## ACKNOWLEDGMENTS

We would like to thank the Air Force Office of Scientific research which made this work possible through Grant No. F49620-94-1-0141. D.J.M. acknowledges the NSF for a graduate fellowship. M.S. would like to thank the Mitsubishi Chemical Corporation for supporting his participation in this research.

<sup>1</sup>J. S. Bader and B. J. Berne, *J. Chem. Phys.* **100**, 8359 (1994).

<sup>2</sup>D. W. Oxtoby, *Adv. Chem. Phys.* **47**, 487 (1981).

<sup>3</sup>R. S. Urdahl, K. D. Rector, D. J. Myers, P. H. Davis, and M. D. Fayer, *J. Chem. Phys.* **105**, 8973 (1996).

<sup>4</sup>R. S. Urdahl, D. J. Myers, K. D. Rector, P. H. Davis, B. J. Cherayil, and M. D. Fayer, *J. Chem. Phys.* **107**, 3747 (1997).

<sup>5</sup>B. J. Cherayil and M. D. Fayer, *J. Chem. Phys.* **107**, 7642 (1997).

<sup>6</sup>D. Schwarzer, J. Troe, and M. Zerezke, *J. Chem. Phys.* **107**, 8380 (1997).

<sup>7</sup>D. J. Myers, R. S. Urdahl, B. J. Cherayil, and M. D. Fayer, *J. Chem. Phys.* **107**, 9741 (1997).

<sup>8</sup>M. E. Paige and C. B. Harris, *Chem. Phys.* **149**, 37 (1990).

<sup>9</sup>J. K. Brown, C. B. Harris, and J. C. Tully, *J. Chem. Phys.* **89**, 6687 (1988).

<sup>10</sup>S. A. Egorov and J. L. Skinner, *J. Chem. Phys.* **105**, 7047 (1996).

<sup>11</sup>A. Tokmakoff, C. D. Marshall, and M. D. Fayer, *J. Opt. Soc. Am. B* **10**, 1785 (1993).

<sup>12</sup>V. M. Kenkre, A. Tokmakoff, and M. D. Fayer, *J. Chem. Phys.* **101**, 10618 (1994).

<sup>13</sup>D. W. Oxtoby, *Annu. Rev. Phys. Chem.* **32**, 77 (1981).

<sup>14</sup>P. Moore, A. Tokmakoff, T. Keyes, and M. D. Fayer, *J. Chem. Phys.* **103**, 3325 (1995).

<sup>15</sup>M. Buchner, B. M. Ladanyi, and R. M. Stratt, *J. Chem. Phys.* **97**, 8522 (1992).

<sup>16</sup>A. Tokmakoff, B. Sauter, and M. D. Fayer, *J. Chem. Phys.* **100**, 9035 (1994).

<sup>17</sup>J. G. Kirkwood and F. P. Buff, *J. Chem. Phys.* **19**, 774 (1951).

<sup>18</sup>H. E. Stanley, *Introduction to Phase Transitions and Critical Phenomena* (Oxford, New York, 1971).

<sup>19</sup>NIST Standard Reference Data Base 14, 9.08 ed. (U.S. Department of Commerce, Boulder, CO, 1992).

<sup>20</sup>A. Tokmakoff and M. D. Fayer, *J. Chem. Phys.* **103**, 2810 (1995).

<sup>21</sup>S. Tucker (private communication, 1998).

<sup>22</sup>B. Cherayil and M. D. Fayer (unpublished).

<sup>23</sup>Due to a modification of our fitting routine, as well as additional data, some of the lifetime values reported in Ref. 4, Fig. 4, (ethane solvent only) have been changed, particularly those at 34 °C. This does not significantly alter the nature of the plateau region observed in Ref. 4, but rather shifts the lifetimes to longer times. The lifetime at 5 mol/ℓ is ~30 ps longer and the lifetime at 12 mol/ℓ is ~20 ps longer. The values between these two densities are ~10 to ~15 ps longer. The result is to make the plateau in the lifetime with density that occurs around the critical density slightly less flat on the low density side, and somewhat flatter on the high density side. The data point in ethane at 5 mol/ℓ and 50 °C has a shorter lifetime by 25 ps than is reported in Ref. 4. The reduction in lifetime brings this point more in line with the other 50 °C data reported in Ref. 4. The other points at 50 °C are essentially unchanged.